

GPT-Prompt Controlled Diffusion for Weakly-Supervised Semantic Segmentation

Wangyu Wu^{1,2†}, Tianhong Dai^{3†}, Xiaowei Huang², Fei Ma^{1*}, Jimin Xiao^{1*}

¹Xi’an Jiaotong-Liverpool University ²The University of Liverpool ³University of Aberdeen

*

Abstract

Weakly supervised semantic segmentation (WSSS), aiming to train segmentation models solely using image-level labels, has received significant attention. Existing approaches mainly concentrate on creating high-quality pseudo labels by utilizing existing images and their corresponding image-level labels. However, the quality of pseudo labels degrades significantly when the size of available dataset is limited. Thus, in this paper, we tackle this problem from a different view by introducing a novel approach called *GPT-Prompt Controlled Diffusion* (GPCD) for data augmentation. This approach enhances the current labeled datasets by augmenting with a variety of images, achieved through controlled diffusion guided by GPT prompts. In this process, the existing images and image-level labels provide the necessary control information, where GPT is employed to enrich the prompts, leading to the generation of diverse backgrounds. Moreover, we integrate data source information as tokens into the Vision Transformer (ViT) framework. These tokens are specifically designed to improve the ability of downstream WSSS framework to recognize the origins of augmented images. Our proposed GPCD approach clearly surpasses existing state-of-the-art methods. This effect is more obvious when the amount of available data is small, demonstrating the effectiveness of our method. Our source code will be released.

1 Introduction

Semantic segmentation, a crucial task in computer vision, focuses on delineating target objects at the pixel level. With the recent advances in deep learning, fully supervised semantic segmentation (FSSS) models have achieved notable progress [Chen *et al.*, 2017; Yuan *et al.*, 2020; Xie *et al.*, 2021]. However, acquiring sufficient pixel-level annotations for segmentation is notably expensive and time-consuming when compared to other vision tasks like classification and object de-

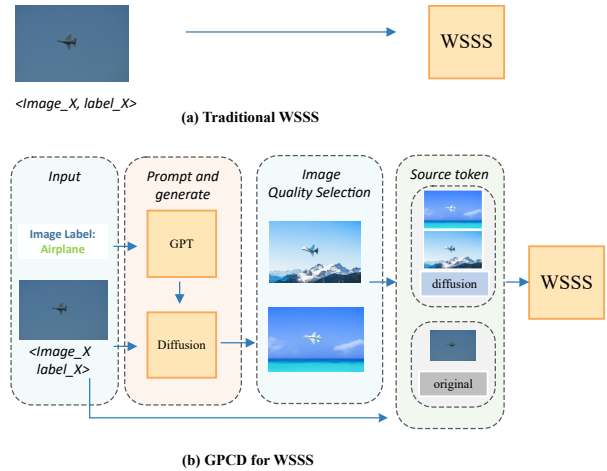


Figure 1: (a) Previous WSSS approaches solely relied on images sourced exclusively from the original dataset for training purposes. (b) Our proposed GPCD utilizes GPT with image labels as input to generate diverse prompts. Subsequently, we use the diffusion model to generate synthetic images. Next, an image selection module is employed to annotate and select high-quality synthetic images for augmenting the original dataset during training. Finally, we combine the augmented data with the original dataset, incorporating source signals into the WSSS task.

tection. In recent times, there has been a substantial focus on weakly supervised semantic segmentation (WSSS) to mitigate the dependency on pixel-level annotations by leveraging “weak” labels, including image-level labels [Ahn and Kwak, 2018], points [Bearman *et al.*, 2016], scribbles [Lin *et al.*, 2016] and bounding boxes [Lee *et al.*, 2021a]. Among these approaches, image-level WSSS has gained popularity due to the ease of obtaining image-level annotations, and in this paper, we also embrace this image-level setting.

Weakly-supervised semantic segmentation utilizes image-level labels to generate pixel-level pseudo labels for training segmentation models. The primary challenge lies in improving the quality of these generated pseudo labels. Currently, mainstream methods mainly focus on enhancing network architectures and analyzing existing data [Chang *et al.*, 2020; Ru *et al.*, 2023; Wu *et al.*, 2023]. This includes exploring sub-class distinctions [Chang *et al.*, 2020]. Notably, the method presented in [Ru *et al.*, 2023] incorporates a con-

*Corresponding authors. †Contributed equally to this work.

trastive learning loss for intra-class compactness and inter-class separability. Alternatively, efforts are directed towards optimizing network structures to better learning in weakly-supervised scenarios [Rossetti *et al.*, 2022; Xu *et al.*, 2022; Ru *et al.*, 2022]. However, it is important to note that the methods mentioned above are all limited by the scale of the available training data.

To address this issue, we propose *GPT-Prompt Controlled Diffusion* (GPCD), for effective data augmentation that integrates knowledge from multiple pre-trained models. GPCD incorporates multiple steps, including: *GPT Prompt*, *Diffusion Generate*, *High-quality Image Selection*, and *Source Information Tokens for WSSS training*.

The primary motivation behind GPCD is to utilize the GPT prompt and controlled diffusion capabilities to generate a larger and more diverse set of images to enhance the performance of WSSS tasks.

In detail, we complete our method through four steps: 1) Prompt. We use GPT-3.5 [Ouyang *et al.*, 2022] with image labels as input and generate rich background textual prompts for the diffusion model Stable Diffusion [Romach *et al.*, 2022] with ControlNet [Zhang and Agrawala, 2023] based on certain templates. With GPT-driven prompt, we obtain diverse and more reasonable background textual prompts, rather than being limited to prompts from a single background. 2) Generate. We employ ControlNet [Zhang and Agrawala, 2023] to generate additional images based on the original image and prompts generated by GPT modules, thereby expanding the training data without additional manpower for collection and annotation. 3) High-Quality Image Selection. We train an image classifier with existing image-level labels and predict category probabilities for images augmented by diffusion. We select images with high prediction scores as high-quality images and discard those with low prediction scores to ensure the quality of the enhanced dataset, avoiding introducing noise into downstream WSSS tasks. 4) Source Information Tokens. We differentiate diffusion images from original images by adding source tokens to the ViT-based framework. This allows downstream WSSS tasks to better perceive information from different data sources. GPCD can generate various new images to enhance WSSS task datasets, improving WSSS performances.

In this paper, we propose GPCD to generate high-quality synthetic training data for WSSS (see Figure 1). Our contributions are:

- 1) Our approach is the first proposal to utilize conditional diffusion with GPT prompts to generate a more diverse set of images for augmenting the original dataset with image-level labels, so as to enhance WSSS performance.
- 2) We introduce an image selection approach designed to retain high-quality generated data while filtering out low-quality generated images. This strategy prevents negative impact on model training with noisy images.
- 3) We propose to use data source information as tokens that explicitly indicate whether an image is from the original training data or the diffusion-generated data to further enrich the data augmentation approach for the WSSS framework. By incorporating these additional source to-

kens into the ViT tokens, we empower the downstream WSSS framework to better capture different behaviors from the specific data sources to improve the overall performance of the framework.

- 4) Our proposed framework outperforms all current state-of-the-art methods, and it shows varying performance improvements across different training data sizes, particularly at 5% of the training data, where there is 5.3% increase for the segmentation task on the validation set on the PASCAL VOC 2012 dataset.

2 Related Work

2.1 Weakly-Supervised Semantic Segmentation

Weakly Supervised Semantic Segmentation (WSSS) using image-level labels typically generates CAM as the initial pseudo labels. Many methods are exploring how to address the drawbacks of CAM, which usually only activates the most discriminative object regions. For example, methods like erasing [Wei *et al.*, 2017], online attention accumulation [Jiang *et al.*, 2019], and cross-image semantic mining [Sun *et al.*, 2020] have been proposed. [Lee *et al.*, 2021b; Yao *et al.*, 2021] utilize additional saliency maps as supervision to suppress background regions and mine non-salient objects. [Chen *et al.*, 2022; Du *et al.*, 2022] encourage integral activation of object regions by contrasting pixel and prototype representations. The method [Chang *et al.*, 2020] also involves injecting more category information into the network or performing additional information learning on existing training data. Some recent works also introduce ViT to WSSS, with models like MCTformer [Xu *et al.*, 2022], AFA [Ru *et al.*, 2022], although both still rely on the use of CAM. MCTformer leverages attention mechanism of ViT to generate localization maps and employs PSA [Ahn and Kwak, 2018] for pseudo labels generation. AFA employs multi-head self-attention of ViT for global insights and an affinity module to propagate pseudo labels. ViT-PCM [Rossetti *et al.*, 2022] begins to explore the use of ViT without CAM in WSSS. However, these approaches explore from the perspective of network architecture or the introduction of additional features, limited by the size of the training data. In this paper, we enhance WSSS from the perspective of data augmentation by generating more training data.

2.2 Prompt-based Language Models

Prompt-based learning involves enhancing the performance of pre-trained language models (PLMs) by adding task-specific instructions to the input. Early approaches relied on manually crafted prompts to adapt to different generation tasks [Brown *et al.*, 2020; Raffel *et al.*, 2020; Zou *et al.*, 2021]. However, these manually designed prompts lack flexibility and cannot be easily applied to new tasks. Consequently, recent research has shifted towards automating the generation of prompts [Shin *et al.*, 2020]. Furthermore, some methods [Liu *et al.*, 2023; Li and Liang, 2021] have proposed optimizing continuous prompts to overcome the challenges of optimizing prompts in discrete space, providing greater flexibility across various tasks. Recently, PLMs have also been applied to computer vision tasks, and the method [Zhang

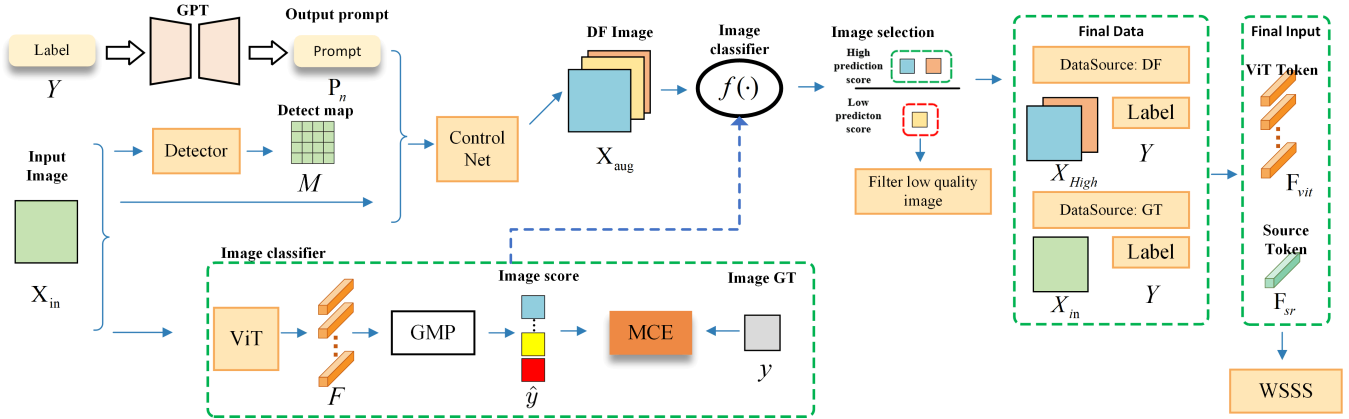


Figure 2: The overall framework of GPCD consists of several steps. Firstly, GPCD utilizes the GPT module to generate a text prompt based on image-level labels. Next, the output from GPT is used in the subsequent diffusion modules, where the diffusion modules use the training data image and GPT output as controlled diffusion input to generate entirely different images. Subsequently, the original image is processed using the ViT as an encoder to generate patch embeddings, and a patch-driven classifier is trained for image categorization. Then, the generated diffusion images are passed through the same trained image classifier to select a high-quality image set. Moreover, the selected image set, along with the original images and their corresponding labels with source tokens, is passed to the downstream WSSS task.

et al., 2023] utilizes prompts to enhance few-shot learners. In contrast, our approach proposes using PLMs to generate prompts to enhance the diversity of image description text. As far as I know, it’s the first time utilizing PLMs to generate diverse prompts for enhancing the WSSS task.

2.3 Diffusion Probabilistic Model

The Diffusion Probabilistic Model (DPM) was first introduced in [Sohl-Dickstein *et al.*, 2015], which have recently gained prominence in computer vision [Ho *et al.*, 2020; Song *et al.*, 2020a; Song *et al.*, 2020b]. The DPMs demonstrate strong capabilities in image generation, as they can generate images with high quality, minimal artifacts, effectively corresponding to the provided text prompts. Noteworthy recent advances, such as Stable Diffusion [Rombach *et al.*, 2022] with ControlNet [Zhang and Agrawala, 2023], further enhance the ability to produce high-quality synthetic images. By leveraging the advantages of diffusion models, we propose the GPCD method, which is the first work to adapt conditional DPMs with a GPT prompt for the WSSS task.

3 Methodology

In this section, we outline the fundamental framework and key components of our proposed GPCD method. Initially, we introduce the overall architecture and workflow (Section 3.1). Following that, we discuss how we employ GPT and a diffusion model for image data augmentation in WSSS tasks (Section 3.2). Additionally, we develop a high-quality image selection strategy to ensure the quality of the data generated by the diffusion model, thereby reducing model noise (Section 3.3). Finally, we describe the details of the final augmented dataset, which utilizes multiple data source tokens for training (Section 3.4).

3.1 Overall Structure

As illustrated in Figure 2, we first adopt the GPT-3.5 model [Ouyang *et al.*, 2022] to produce textual prompts for the sub-

sequent diffusion model with a pre-defined template as a basis. We then utilize the diffusion model [Rombach *et al.*, 2022], in conjunction with ControlNet [Zhang and Agrawala, 2023], to generate synthetic training samples, which leverages original images and GPT-generated prompts with label information as inputs. In addition, we train a ViT-based image classifier [Dosovitskiy *et al.*, 2020], using an existing dataset with image-level labels, to select high-quality generated training samples. During this selection process, we identify generated images with high prediction scores as high-quality samples, while filtering out low-quality images characterized by noise. Finally, we augment the original dataset with these generated samples and integrate the data source information as the source token for training in WSSS.

3.2 Image Augmentation: Prompt and Generation

Prompt with GPT. In the WSSS setting, we denote training images as X_{in} and their corresponding labels as Y . As depicted in Figure 2, for each of the N categories involved in the dataset, a pre-defined template is served as language commands for GPT-3.5 [Ouyang *et al.*, 2022] to generate text prompts, which ensures the relevance and variety of language commands.

$$P_n = \text{GPT-3.5}(\text{commands}), \quad (1)$$

where P_n is the text prompt for generating synthetic samples of category n , and it is used as the input for ControlNet. For each specific category, we design a unified template as the input command for GPT to replace the background of the original training images with a rational one, which only requires image-level labels. For instance, the template is designed as “Generate prompts for diverse and reasonable backgrounds for airplane images generated using the diffusion model. Provide ten different background prompts following the pattern airplane in [background], with [background] replaced by the actual background.”.

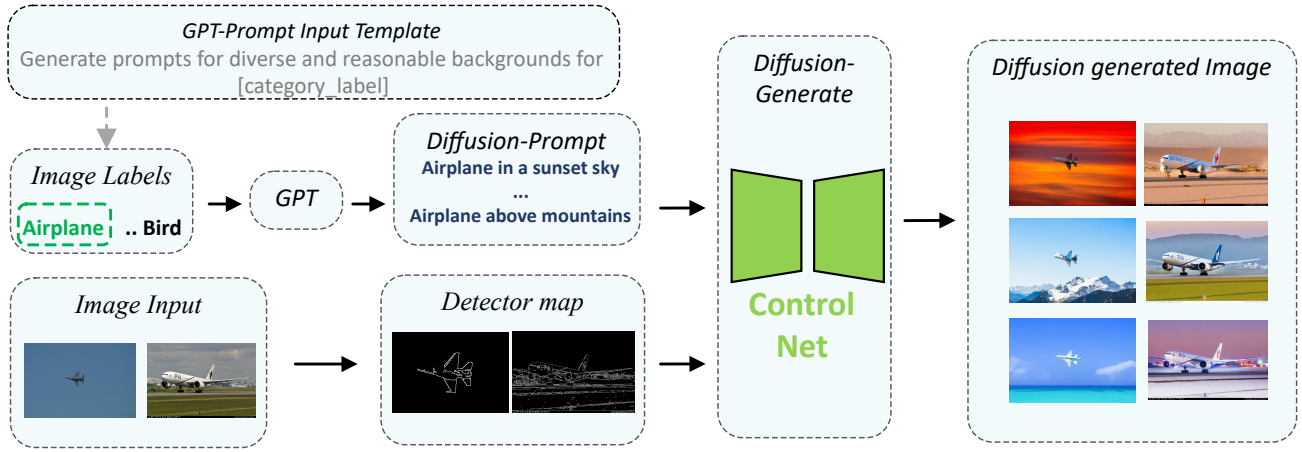


Figure 3: The prompt and generate pipeline of our GPCD. The airplane in the showcase is using the diffusion model with prompts to generate candidate images. Subsequently, these candidate images will be filtered through image selection to ensure that only high-quality images will be used as training data for the downstream WSSS.

Generation via diffusion. The motivation for employing controlled image diffusion models in data augmentation lies in their capability to generate an unlimited task-specific synthetic images. As illustrated in Figure 3, these augmented images are produced based on a specific image with a corresponding text prompt generated by GPT-3.5. For example, if the image-level label of the original selected image is “airplane”, then the output of GPT is a text prompt that includes the image-label and a generated background, such as “airplane in the sky”. Both the selected training image and the generated text prompt are used as the inputs for the diffusion model. In the right-hand side of Figure 3, we can generate unlimited airplane images with different backgrounds (e.g., mountain, island, and sunset). In this work, we specifically utilize Stable Diffusion with ControlNet (SDC)[Zhang and Agrawala, 2023] as the generative model, with the details illustrated in Figure 2. During the data augmentation phase, an input image $X_{in} \in \mathbb{R}^{h \times w \times 3}$, accompanied by a text prompt P_n and a detection map M , are fed into the SDC model $\delta(\cdot)$ to synthesize augmented training data, denoted as X_{aug} . Specifically, the text prompt is derived from the image-level label Y . The detection map is an extra condition (e.g., Canny Edge [Canny, 1986] and Openpose [Cao *et al.*, 2021]) to control the generation results.

$$X_{aug} = \delta(X_{in}, M, P_n). \quad (2)$$

More details about the data augmentation process are described in Algorithm 1.

3.3 High-quality Synthetic Image Selection

In order to guarantee the quality of synthetic data that will be used for training, a selection strategy is introduced to select the high-quality generated samples. As shown in Figure 2, a ViT-based patch-driven classifier is first trained by using the original dataset with the image-level labels. To train the classifier, the input image X_{in} is divided into s input patches $X_{patch} \in \mathbb{R}^{d \times d \times 3}$ with the fixed size, where $s = \frac{hw}{d^2}$. Then, the patch embedding $F \in \mathbb{R}^{s \times e}$ is achieved by using ViT

Algorithm 1: Diffusion Model for Data Augmentation

Input: an input image X_{in} , a prompt P with image label Y
Output: a generated image X_{aug}

- 1 $P \leftarrow \text{generate_prompt}(Y)$
- 2 **if** “person” $\in Y$ **then**
- 3 $M \leftarrow \text{detect_map}(X_{in}, \text{human_pose})$
- 4 **else**
- 5 $M \leftarrow \text{detect_map}(X_{in}, \text{canny_edge})$
- 6 $X_{aug} \leftarrow \delta(X_{in}, M, P)$

encoder. Next, a weight $W \in \mathbb{R}^{e \times |\mathcal{C}|}$ and a softmax function is applied to output the prediction scores $Z \in \mathbb{R}^{s \times |\mathcal{C}|}$ of each patch:

$$Z = \text{softmax}(FW), \quad (3)$$

where \mathcal{C} is the set of categories in the dataset. Global maximum pooling (GMP) is then used to select the highest prediction scores $\hat{y} \in \mathbb{R}^{1 \times |\mathcal{C}|}$ in each class among all patches. Finally, \hat{y} is utilized as the prediction scores for the image-level classification and the classifier is trained via using the multi-label classification prediction error (MCE):

$$\begin{aligned} \mathcal{L}_{MCE} &= \frac{1}{|\mathcal{C}|} \sum_{c \in \mathcal{C}} BCE(y_c, \hat{y}_c) \\ &= -\frac{1}{|\mathcal{C}|} \sum_{c \in \mathcal{C}} y_c \log(\hat{y}_c) + (1 - y_c) \log(1 - \hat{y}_c), \end{aligned} \quad (4)$$

where, \hat{y}_c is the prediction score of class c and y_c is the ground-truth label. Once the classifier finishes the training, we can use it to select the high-quality generated training data.

In the selection stage, the synthetic image X_{aug} generated by $\langle X_{in}, Y \rangle$, is passed into the classifier, followed by the GMP to output the image-level prediction score \hat{y} . Then, the classes with the scores above a certain threshold ϵ are used as the ground-truth label for the generated image: $Y_{aug} =$

$\{c | \hat{y}_c > \epsilon\}$. If Y_{aug} is a subset of the label of the input image Y , the generated sample $\langle X_{aug}, Y_{aug} \rangle$ will be added into the synthetic dataset \mathcal{D}_{aug} . More details about the image selection are described in Algorithm 2.

Algorithm 2: High-Quality Image Selection

Input: a ground-truth label of the input image Y , a generated image X_{aug} , a prediction score \hat{y} , a label of generated image Y_{aug} , a set of classes \mathcal{C} , a threshold ϵ and a synthetic dataset \mathcal{D}_{aug}

Output: a synthetic dataset \mathcal{D}_{aug}

```

1  $Y_{aug} \leftarrow \emptyset$ 
2 foreach  $c \in \mathcal{C}$  do
3   if  $\hat{y}_c > \epsilon$  then
4      $Y_{aug} \leftarrow Y_{aug} \cup \{c\}$ 
5 if  $Y_{aug} \subseteq Y$  then
6    $\mathcal{D}_{aug} \leftarrow \mathcal{D}_{aug} \cup \{\langle X_{aug}, Y_{aug} \rangle\}$ 

```

This selection strategy serves two purposes. First, it only keeps the synthetic samples with high prediction scores in specific categories, which guarantees there is a high probability that objects of these classes will appear in the synthetic image. Second, the synthetic image will not contain objects that do not belong to the image-level label of the input image. In this way, the quality of synthetic dataset \mathcal{D}_{aug} can be improved.

3.4 Final Training Dataset of WSSS

After selecting the high-quality generated training samples, the synthetic dataset \mathcal{D}_{aug} and the original dataset \mathcal{D}_{origin} are combined as an extended dataset \mathcal{D}_{final} for the training of WSSS:

$$\mathcal{D}_{final} = \mathcal{D}_{origin} \cup \mathcal{D}_{aug}. \quad (5)$$

When using the final dataset for training, there are two alternatives available, both of which can effectively leverage the original and synthetic data, thereby improving the segmentation results.

Option 1: The first option simply treats data from all sources (*i.e.*, original and generated data) equally and uses them directly as training inputs so that they can be adapted to all existing WSSS frameworks without any additional changes.

Option 2: The second option requires a further pre-processing for the input data involves using data source information as tokens that explicitly indicate the data source of the image to provide extra information. As shown in Figure 2, we first extract image embedding tokens F_{ViT} using a ViT encoder, then we utilize another token to represent the data source information of the input image, referred to as F_{sr} . The motivation for adding data source information is to enable the model to more effectively distinguish and process data from different sources. Next, these two tokens are concatenated together to produce a composite token which captures both image feature information and data source information. This composite token serves as the enriched input for

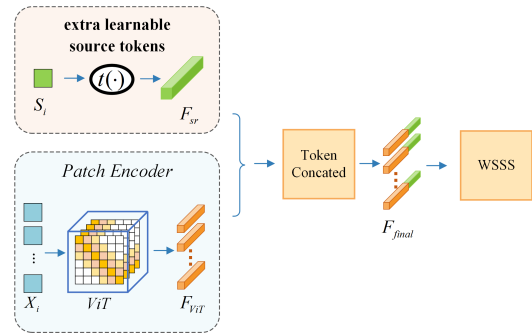


Figure 4: The details about the process of incorporating source tokens with ViT patch tokens as final input tokens.

the WSSS framework that provide additional source-specific insights. After incorporating source tokens, the model allows for different behaviors in images from distinct data source. This enables the model to learn not only shared classification weights but also to learn customize source-adaptive weights during the training process. The model can implicitly learn to extract more relevant information from the data source, adapting to the unique characteristics of each source. This approach improves the model’s accuracy when dealing with specific data sources.

The details are included in Figure 4. For each source information S_i , a function $t(\cdot)$ that contains a learnable variable, is then employed to transform the source information into one of two different tokens accordingly: $F_{sr} \in \{F_{sr}^{origin}, F_{sr}^{synthetic}\} \in \mathbb{R}^{q \times L}$. The dimensionality of F_{sr} is $\mathbb{R}^{1 \times L}$, where L is the length of the source token. For each original image X_{in} , we use a ViT encoder to obtain the feature embedding $F_{ViT} \in \mathbb{R}^{s \times e}$, where s is the number of patches, and e is the patch embedding length. Then, for each patch, we concatenate the source information embedding F_{sr} and the feature embedding F_{ViT} to formulate the final composite embedding F_{final} . Thus, $F_{final} \in \mathbb{R}^{s \times (e+L)}$ provides independent weights for the data source. When combined with source token information, it allows the WSSS framework to better perceive source information, further enhancing the effectiveness of data augmentation and the overall segmentation performance. In summary, either option can effectively improve the WSSS performance.

4 Experiment

4.1 Experimental Settings

Dataset and Evaluation Metric. We conduct our experiments on PASCAL VOC 2012 [Everingham *et al.*, 2010], which comprises 21 categories, and MS COCO 2014 [Lin *et al.*, 2014], which comprises 81 categories, both including an additional background class. The PASCAL VOC 2012 Dataset is typically augmented with the SBD dataset [Hariharan *et al.*, 2011]. In PASCAL VOC 2012, we utilize 10,582 images with image-level annotations for training, and 1,449 images for validation. For MS COCO 2014 dataset, the train and validation set consist of about 82k and 40k images, respectively. The training set contains images with only image-level labels. We report the mean Intersection-Over-Union



Figure 5: Visualizations of ControlNet Generated Images include original training data and augmented images from PASCAL VOC 2012 and MS COCO 2014. (a) depicts the PASCAL VOC 2012 dataset, while (b) displays the MS COCO 2014 dataset. On the left are the original training images, and on the right are the results generated by diffusion with prompts.

(mIoU) as the evaluation criterion. Additionally, we also evaluate the performances of our GPCD method when the amount of original training data is gradually reduced from 10,582 (100%) to 529 (5%) in PASCAL VOC 2012.

Implementation Details. Our GPCD integrates the knowledge from pre-trained GPT-3.5 [Ouyang *et al.*, 2022], Stable Diffusion [Rombach *et al.*, 2022] and ControlNet [Zhang and Agrawala, 2023]. We utilize the ViT-B/16 as ViT model and incorporated the stable diffusion model with ControlNet as our chosen diffusion model and GPT-3.5 as our PLMs model to generate prompt for image generation. To facilitate the training of the patch-driven image classifier, images are resized to 384×384 pixels [Kolesnikov and Lampert, 2016], and the 24×24 encoded patch features are preserved as input. The model undergoes training with a batch size of 16 for a maximum of 80 epochs, employing an image selection threshold $\epsilon = 0.9$. The source token length L is set to 12. The ControlNet utilize Canny Edge [Canny, 1986] and Openpose [Cao *et al.*, 2021] as detectors, and a total of 20 diffusion steps are performed. Due to constraints in computational resources, we augment our dataset by generating an additional 32k images based on the PASCAL VOC 2012 train set using a diffusion model and 82k images based on the MS COCO 2014 train set in the experiments. In the WSSS training stage, our synthetic dataset is seamlessly integrated with the original training dataset to form the final training dataset with source information as token. Subsequently, we select ViT-PCM [Rossetti *et al.*, 2022] as our WSSS framework without any modifications for option 1, and only modify the ViT patch embedding to combine with the source token for option

2. Our final training dataset serves as input for the WSSS framework, while keeping all other settings consistent with ViT-PCM [Rossetti *et al.*, 2022]. The experiments are conducted using two NVIDIA 4090 GPUs. Finally, we use the same verification task and settings as ViT-PCM [Rossetti *et al.*, 2022].

4.2 Generated Image Visualization

As depicted in Figure 5, (a) shows the data augmentation results for PASCAL VOC 2012, while (b) displays the data augmentation results for MS COCO 2014. The images on the left represent the original training data, while those on the right depict the images enhanced by the diffusion model. ControlNet utilizes the original images and a text prompt as input. Upon observing Figure 5, we note that diffusion with a GPT prompt can effectively control the target images. Thus the generated images exhibit certain degree of similarity to the original images while also producing entirely different images, thus preventing them from being overly uniform and enhancing their diversity.

Percentage of Train Data	Baseline on Val	GPCD on Val
5%	62.6%	67.9% +5.3%
50%	68.2%	71.5% +3.3%
100%	69.3%	72.4% +3.1%

Table 1: The comparison of segmentation performances with different sizes of training data on PASCAL VOC 2012.

4.3 Final Segmentation Performance

Comparison of Different Data Percentages. Our proposed GPCD method can effectively increase the effective size of the original training dataset. As reported in Table 1, this enhancement notably enhances the segmentation performances of the downstream WSSS framework. Particularly noteworthy is the amplified impact observed when the training data is limited, such as in the case of only 5% of the dataset, where we achieved a 5.3% performance boost on PASCAL VOC 2012. These findings highlight the high efficacy of our approach in augmenting datasets and improving performances, especially in scenarios with limited training data.

Percentage of Train Data	Model	Pub.	mIoU (%) on Val
100%	MCTformer [Xu <i>et al.</i> , 2022]	CVPR22	61.7
100%	PPC [Du <i>et al.</i> , 2022]	CVPR22	61.5
100%	SIPE [Chen <i>et al.</i> , 2022]	CVPR22	58.6
100%	AFA [Ru <i>et al.</i> , 2022]	CVPR22	63.8
100%	ViT-PCM [Dosovitskiy <i>et al.</i> , 2020]	ECCV22	69.3
100%	USAGE [Peng <i>et al.</i> , 2023]	ICCV23	71.9
100%	SAS [Kim <i>et al.</i> , 2023]	AAAI23	69.5
100%	TSCD [Xu <i>et al.</i> , 2023]	AAAI23	67.3
100%	ToCo [Ru <i>et al.</i> , 2023]	CVPR23	70.5
50%	GPCD (Ours) + ViT-PCM		71.5
100%	GPCD (Ours) + ViT-PCM		72.4

Table 2: The comparison of final semantic segmentation performances on PASCAL VOC 2012.

Percentage of Train Data	Model	Pub.	mIoU (%) on Val
100%	MCTformer [Xu <i>et al.</i> , 2022]	CVPR22	42.0
100%	SIPE [Chen <i>et al.</i> , 2022]	CVPR22	43.6
100%	AFA [Ru <i>et al.</i> , 2022]	CVPR22	38.9
100%	ViT-PCM [Dosovitskiy <i>et al.</i> , 2020]	ECCV22	45.0
100%	ToCo [Ru <i>et al.</i> , 2023]	CVPR23	42.3
100%	OCR [Cheng <i>et al.</i> , 2023]	CVPR23	42.5
100%	SAS [Kim <i>et al.</i> , 2023]	AAAI23	44.8
100%	TSCD [Xu <i>et al.</i> , 2023]	AAAI23	40.1
100%	USAGE [Peng <i>et al.</i> , 2023]	ICCV23	44.3
50%	GPCD (Ours) + ViT-PCM		45.2
100%	GPCD (Ours) + ViT-PCM		45.8

Table 3: The comparison of final semantic segmentation performances on MS COCO 2014.

Backbone	Original Train	diffusion augmentation with GPT prompt	Image Selection	Data Source Info Token	Result on Val
ViT-B/16	✓				69.3%
ViT-B/16	✓	✓			69.0%
ViT-B/16	✓	✓	✓ (option 1)		71.6%
ViT-B/16	✓	✓	✓	✓ (option 2)	72.4%

Table 4: Ablation study on the data augmentation module, the high-quality image selection module, and the source information as token module in PASCAL VOC 2012. Options 1 and option 2, as mentioned in Section 3.4, are highlighted.

Comparison with State-of-the-arts. To evaluate our methods, we applied our approach to the state-of-the-art ViT-PCM as upstream data augmentation while maintaining consistency with the existing ViT-PCM for downstream WSSS. We then compared the segmentation results with state-of-the-art techniques, as shown in Table 2 and Table 3. In PASCAL VOC 2012, even with only 50% of the training data, our method outperforms the baseline ViT-PCM [Dosovitskiy *et al.*, 2020]. In the MS COCO 2014 evaluation, similar results were observed, affirming the effectiveness of our data aug-



Figure 6: The comparison of qualitative segmentation results with baseline (ViT-PCM).

mentation method for this dataset, surpassing both the baseline and current state-of-the-art approaches. The qualitative comparison of segmentation results is illustrated in Figure 6.

4.4 Ablation Studies

We conducted an ablation study to assess the impact of our three key contributions: diffusion augmentation with prompt, high-quality image selection, and multiple source tokens. As shown in Table 4, our diffusion augmentation with prompt introduces some randomly generated noisy images from the diffusion model with prompt, resulting in a 0.3% decrease in mIoU on the validation set. Additionally, the proposed high-quality image selection effectively reduces noisy images by filtering out low-quality ones. This approach leads to a 2.3% improvement in mean Intersection over Union (mIoU) for the baseline Weakly Supervised Semantic Segmentation (WSSS) framework. This improvement corresponds to what we introduced in Section 3.4 as *Option 1*, which involves the direct use of augmented data for WSSS. Finally, *Option 2* in Section 3.4, which incorporates data source information as tokens into the framework, enhances the framework’s ability to perceive and utilize data source information. This results in a further 0.8% performance improvement. When these three methods are combined, our comprehensive approach significantly outperforms the original framework.

5 Conclusion

In this study, we introduce the GPCD approach for data augmentation in weakly supervised semantic segmentation. Unlike previous methods that focus on optimizing network structures or mining information from existing images, our approach integrates a diffusion model-based module with GPT-prompt to augment additional training data. To ensure the quality of the generated images, we propose a high-quality image selection module. Finally, we enhance the augmentation information further by introducing data source information as tokens. By combining these components, our approach demonstrates superior performance compared to other state-of-the-art methods on the PASCAL VOC 2012 and MS COCO 2014 datasets.

References

- [Ahn and Kwak, 2018] Jiwoon Ahn and Suha Kwak. Learning pixel-level semantic affinity with image-level supervision for weakly supervised semantic segmentation. In *Proc. IEEE Conf. Comput. Vis. Pattern Recog.*, pages 4981–4990, 2018.
- [Bearman *et al.*, 2016] Amy Bearman, Olga Russakovsky, Vittorio Ferrari, and Li Fei-Fei. What’s the point: Semantic segmentation with point supervision. In *Eur. Conf. Comput. Vis.*, pages 549–565. Springer, 2016.
- [Brown *et al.*, 2020] Tom Brown, Benjamin Mann, Nick Ryder, Melanie Subbiah, Jared D Kaplan, Prafulla Dhariwal, Arvind Neelakantan, Pranav Shyam, Girish Sastry, Amanda Askell, et al. Language models are few-shot learners. *Advances in Neural Information Processing Systems*, 33:1877–1901, 2020.
- [Canny, 1986] John Canny. A computational approach to edge detection. *IEEE Trans. Pattern Anal. Mach. Intell.*, PAMI-8(6):679–698, 1986.
- [Cao *et al.*, 2021] Zhe Cao, Gines Hidalgo, Tomas Simon, Shih-En Wei, and Yaser Sheikh. Openpose: Realtime multi-person 2d pose estimation using part affinity fields. *IEEE Trans. Pattern Anal. Mach. Intell.*, 43(1):172–186, 2021.
- [Chang *et al.*, 2020] Yu-Ting Chang, Qiaosong Wang, Wei-Chih Hung, Robinson Piramuthu, Yi-Hsuan Tsai, and Ming-Hsuan Yang. Weakly-supervised semantic segmentation via sub-category exploration. In *Proc. IEEE Conf. Comput. Vis. Pattern Recog.*, pages 8991–9000, 2020.
- [Chen *et al.*, 2017] Liang-Chieh Chen, George Papandreou, Iasonas Kokkinos, Kevin Murphy, and Alan L Yuille. Deeplab: Semantic image segmentation with deep convolutional nets, atrous convolution, and fully connected crfs. *IEEE Trans. Pattern Anal. Mach. Intell.*, 40(4):834–848, 2017.
- [Chen *et al.*, 2022] Qi Chen, Lingxiao Yang, Jian-Huang Lai, and Xiaohua Xie. Self-supervised image-specific prototype exploration for weakly supervised semantic segmentation. In *Proc. IEEE Conf. Comput. Vis. Pattern Recog.*, pages 4288–4298, 2022.
- [Cheng *et al.*, 2023] Zesen Cheng, Pengchong Qiao, Kehan Li, Siheng Li, Pengxu Wei, Xiangyang Ji, Li Yuan, Chang Liu, and Jie Chen. Out-of-candidate rectification for weakly supervised semantic segmentation. In *Proc. IEEE Conf. Comput. Vis. Pattern Recog.*, pages 23673–23684, 2023.
- [Dosovitskiy *et al.*, 2020] Alexey Dosovitskiy, Lucas Beyer, Alexander Kolesnikov, Dirk Weissenborn, Xiaohua Zhai, Thomas Unterthiner, Mostafa Dehghani, Matthias Minderer, Georg Heigold, Sylvain Gelly, et al. An image is worth 16x16 words: Transformers for image recognition at scale. *arXiv preprint arXiv:2010.11929*, 2020.
- [Du *et al.*, 2022] Ye Du, Zehua Fu, Qingjie Liu, and Yunhong Wang. Weakly supervised semantic segmentation by pixel-to-prototype contrast. In *Proc. IEEE Conf. Comput. Vis. Pattern Recog.*, pages 4320–4329, 2022.
- [Everingham *et al.*, 2010] Mark Everingham, Luc Van Gool, Christopher KI Williams, John Winn, and Andrew Zisserman. The pascal visual object classes (VOC) challenge. *Int. J. Comput. Vis.*, 88:303–338, 2010.
- [Hariharan *et al.*, 2011] Bharath Hariharan, Pablo Arbeláez, Lubomir Bourdev, Subhransu Maji, and Jitendra Malik. Semantic contours from inverse detectors. In *Proc. IEEE Int. Conf. Comput. Vis.*, pages 991–998, 2011.
- [Ho *et al.*, 2020] Jonathan Ho, Ajay Jain, and Pieter Abbeel. Denoising diffusion probabilistic models. *Advances in Neural Information Processing Systems*, 33:6840–6851, 2020.
- [Jiang *et al.*, 2019] Peng-Tao Jiang, Qibin Hou, Yang Cao, Ming-Ming Cheng, Yunchao Wei, and Hong-Kai Xiong. Integral object mining via online attention accumulation. In *Proc. IEEE Int. Conf. Comput. Vis.*, pages 2070–2079, 2019.
- [Kim *et al.*, 2023] Sangtae Kim, Daeyoung Park, and Byonghyo Shim. Semantic-aware superpixel for weakly supervised semantic segmentation. In *AAAI Conf. Artif. Intell.*, volume 37, pages 1142–1150, 2023.
- [Kolesnikov and Lampert, 2016] Alexander Kolesnikov and Christoph H Lampert. Seed, expand and constrain: Three principles for weakly-supervised image segmentation. In *Eur. Conf. Comput. Vis.*, pages 695–711, 2016.
- [Lee *et al.*, 2021a] Jungbeom Lee, Jihun Yi, Chaehun Shin, and Sungroh Yoon. Bbam: Bounding box attribution map for weakly supervised semantic and instance segmentation. In *Proc. IEEE Conf. Comput. Vis. Pattern Recog.*, pages 2643–2652, 2021.
- [Lee *et al.*, 2021b] Seungho Lee, Minhyun Lee, Jongwuk Lee, and Hyunjung Shim. Railroad is not a train: Saliency as pseudo-pixel supervision for weakly supervised semantic segmentation. In *Proc. IEEE Conf. Comput. Vis. Pattern Recog.*, pages 5495–5505, 2021.
- [Li and Liang, 2021] Xiang Lisa Li and Percy Liang. Prefix-tuning: Optimizing continuous prompts for generation. *arXiv preprint arXiv:2101.00190*, 2021.
- [Lin *et al.*, 2014] Tsung-Yi Lin, Michael Maire, Serge Belongie, James Hays, Pietro Perona, Deva Ramanan, Piotr Dollár, and C Lawrence Zitnick. Microsoft coco: Common objects in context. In *Eur. Conf. Comput. Vis.*, pages 740–755. Springer, 2014.
- [Lin *et al.*, 2016] Di Lin, Jifeng Dai, Jiaya Jia, Kaiming He, and Jian Sun. Scribblesup: Scribble-supervised convolutional networks for semantic segmentation. In *Proc. IEEE Conf. Comput. Vis. Pattern Recog.*, pages 3159–3167, 2016.
- [Liu *et al.*, 2023] Xiao Liu, Yanan Zheng, Zhengxiao Du, Ming Ding, Yujie Qian, Zhilin Yang, and Jie Tang. Gpt understands, too. *AI Open*, 2023.
- [Ouyang *et al.*, 2022] Long Ouyang, Jeffrey Wu, Xu Jiang, Diogo Almeida, Carroll Wainwright, Pamela Mishkin, Chong Zhang, Sandhini Agarwal, Katarina Slama, Alex

- Ray, et al. Training language models to follow instructions with human feedback. *Advances in Neural Information Processing Systems*, 35:27730–27744, 2022.
- [Peng et al., 2023] Zelin Peng, Guanchun Wang, Lingxi Xie, Dongsheng Jiang, Wei Shen, and Qi Tian. Usage: A unified seed area generation paradigm for weakly supervised semantic segmentation. In *Proc. IEEE Int. Conf. Comput. Vis.*, pages 624–634, 2023.
- [Raffel et al., 2020] Colin Raffel, Noam Shazeer, Adam Roberts, Katherine Lee, Sharan Narang, Michael Matena, Yanqi Zhou, Wei Li, and Peter J Liu. Exploring the limits of transfer learning with a unified text-to-text transformer. *The Journal of Machine Learning Research*, 21(1):5485–5551, 2020.
- [Rombach et al., 2022] Robin Rombach, Andreas Blattmann, Dominik Lorenz, Patrick Esser, and Björn Ommer. High-resolution image synthesis with latent diffusion models. In *Proc. IEEE Conf. Comput. Vis. Pattern Recog.*, pages 10684–10695, 2022.
- [Rossetti et al., 2022] Simone Rossetti, Damiano Zappia, Marta Sanzari, Marco Schaerf, and Fiora Pirri. Max pooling with vision transformers reconciles class and shape in weakly supervised semantic segmentation. In *Eur. Conf. Comput. Vis.*, pages 446–463, 2022.
- [Ru et al., 2022] Lixiang Ru, Yibing Zhan, Baosheng Yu, and Bo Du. Learning affinity from attention: End-to-end weakly-supervised semantic segmentation with transformers. In *Proc. IEEE Conf. Comput. Vis. Pattern Recog.*, pages 16846–16855, 2022.
- [Ru et al., 2023] Lixiang Ru, Heliang Zheng, Yibing Zhan, and Bo Du. Token contrast for weakly-supervised semantic segmentation. In *Proc. IEEE Conf. Comput. Vis. Pattern Recog.*, pages 3093–3102, 2023.
- [Shin et al., 2020] Taylor Shin, Yasaman Razeghi, Robert L Logan IV, Eric Wallace, and Sameer Singh. Autoprompt: Eliciting knowledge from language models with automatically generated prompts. *arXiv preprint arXiv:2010.15980*, 2020.
- [Sohl-Dickstein et al., 2015] Jascha Sohl-Dickstein, Eric Weiss, Niru Maheswaranathan, and Surya Ganguli. Deep unsupervised learning using nonequilibrium thermodynamics. In *Int. Conf. Mach. Learn.*, pages 2256–2265, 2015.
- [Song et al., 2020a] Jiaming Song, Chenlin Meng, and Stefano Ermon. Denoising diffusion implicit models. *arXiv preprint arXiv:2010.02502*, 2020.
- [Song et al., 2020b] Yang Song, Jascha Sohl-Dickstein, Diederik P Kingma, Abhishek Kumar, Stefano Ermon, and Ben Poole. Score-based generative modeling through stochastic differential equations. *arXiv preprint arXiv:2011.13456*, 2020.
- [Sun et al., 2020] Guolei Sun, Wenguan Wang, Jifeng Dai, and Luc Van Gool. Mining cross-image semantics for weakly supervised semantic segmentation. In *Eur. Conf. Comput. Vis.*, pages 347–365. Springer, 2020.
- [Wei et al., 2017] Yunchao Wei, Jiashi Feng, Xiaodan Liang, Ming-Ming Cheng, Yao Zhao, and Shuicheng Yan. Object region mining with adversarial erasing: A simple classification to semantic segmentation approach. In *Proc. IEEE Conf. Comput. Vis. Pattern Recog.*, pages 1568–1576, 2017.
- [Wu et al., 2023] Yuanchen Wu, Xiaoqiang Li, Songmin Dai, Jide Li, Tong Liu, and Shaorong Xie. Hierarchical semantic contrast for weakly supervised semantic segmentation. In *IJCAI*, pages 1542–1550, 2023.
- [Xie et al., 2021] Enze Xie, Wenhai Wang, Zhiding Yu, Anima Anandkumar, Jose M Alvarez, and Ping Luo. Segformer: Simple and efficient design for semantic segmentation with transformers. *Advances in Neural Information Processing Systems*, 34:12077–12090, 2021.
- [Xu et al., 2022] Lian Xu, Wanli Ouyang, Mohammed Benamoun, Farid Boussaid, and Dan Xu. Multi-class token transformer for weakly supervised semantic segmentation. In *Proc. IEEE Conf. Comput. Vis. Pattern Recog.*, pages 4310–4319, 2022.
- [Xu et al., 2023] Rongtao Xu, Changwei Wang, Jiayi Sun, Shibiao Xu, Weiliang Meng, and Xiaopeng Zhang. Self correspondence distillation for end-to-end weakly-supervised semantic segmentation. In *AAAI Conf. Artif. Intell.*, volume 37, pages 3045–3053, 2023.
- [Yao et al., 2021] Yazhou Yao, Tao Chen, Guo-Sen Xie, Chuanyi Zhang, Fumin Shen, Qi Wu, Zhenmin Tang, and Jian Zhang. Non-salient region object mining for weakly supervised semantic segmentation. In *Proc. IEEE Conf. Comput. Vis. Pattern Recog.*, pages 2623–2632, 2021.
- [Yuan et al., 2020] Yuhui Yuan, Xilin Chen, and Jingdong Wang. Object-contextual representations for semantic segmentation. In *Eur. Conf. Comput. Vis.*, pages 173–190. Springer, 2020.
- [Zhang and Agrawala, 2023] Lvmin Zhang and Maneesh Agrawala. Adding conditional control to text-to-image diffusion models. *arXiv preprint arXiv:2302.05543*, 2023.
- [Zhang et al., 2023] Renrui Zhang, Xiangfei Hu, Bohao Li, Siyuan Huang, Hanqiu Deng, Yu Qiao, Peng Gao, and Hongsheng Li. Prompt, generate, then cache: Cascade of foundation models makes strong few-shot learners. In *Proc. IEEE Conf. Comput. Vis. Pattern Recog.*, pages 15211–15222, 2023.
- [Zou et al., 2021] Xu Zou, Da Yin, Qingyang Zhong, Hongxia Yang, Zhilin Yang, and Jie Tang. Controllable generation from pre-trained language models via inverse prompting. In *Proceedings of the 27th ACM SIGKDD Conference on Knowledge Discovery & Data Mining*, pages 2450–2460, 2021.